International Hydrographic Review, Monaco, LXXI(2), September 1994

AIRBORNE LASER DEPTH SOUNDING IN SWEDEN

by Kurt KOPPARI, Ulf KARLSSON, Ove STEINVALL[1]

Abstract

This paper will review some of the laser depth sounding work in Sweden. These activities include the development of a helicopter borne lidar called FLASH[1], [2] as well as instrumentation (HOSS) for in situ measurement of the optical water parameters.[3] These instruments have been used in a rather extensive field trial, some of which will be discussed in more detail.

The FLASH system has been further developed into two operational systems called Hawk Eye, with Saab Instruments as the main contractor and Optech Inc. as the main subcontractor. Data from Hawk Eye will hopefully be available at the time of the meeting and will be discussed. FOA is member of the Hawk Eye project team together with the Swedish Hydrographic Department, the Swedish Navy and the Swedish Material Administration (FMV).

INTRODUCTION

Activities in laser depth sounding started in Sweden at the Defence Research Institute during the early seventies. Ship borne measurements were made using a frequency doubled range finder. Penetration depths between 10-20 metres were achieved but the technology for high prf lasers was not mature to enable development of any airborne scanning system. Interest for laser bathymetry increased during the early eighties and airborne trials were performed at low prf (10 Hz).

Maximum penetration down to 20-30 metres was observed and some preliminary tests of bottom profiling were made in cooperation with the Swedish Hydrographic Department[2, 4]. The results were encouraging and FOA was given the task to develop and demonstrate a scanning system with a real time echo extraction

[1] Swedish Defense Research Establishment (FOA), Dept. 3, P.O. Box 1165, Linköping, Sweden.

and a real time depth colour coded display to help the operator. The system was to be helicopter borne. The system work started in 1986 with Optech Inc. delivering the receiver and associated electronics. Saab Instrument developed a programmable scanner[5] which enables the operator to control the scanning pattern, sounding density, etc. The laser was bought from AWA in Australia and was developed for the Australian programme in laser bathymetry.

The system was called FLASH (FOA Laser Airborne Sounder for Hydrography). The system was used in field trials between 1989-1992. Some of the results have been reported in the open literature[2]. This article will show some of the more recent results acquired with FLASH.

In parallel with the laser system development at FOA there was a need for an *in situ* profiling instrumentation to measure relevant water parameters in direct connection with the helicopter trials. A system called HOSS[6] (Hydro Optical Sensor System) was developed. The subsea unit was lowered from the helicopter to get a vertical profile of the water turbidity at several locations in the test area.

Modelling work of the laser system performance was done using both Monte Carlo simulation and analytical models[7,8]. A software package called Scan View[9] has been developed to simplify the post processing.

A smaller effort in gated viewing has also been undertaken to investigate the potential of this technique as a complement for helicopter borne lidar for investigating the sea bed with higher spatial resolution.

At the time of writing most efforts are concentrated on the acceptance test of the Hawk Eye System which has been developed in two versions, one for the Swedish Hydrographic Department and one for the Swedish Navy. The Hawk Eye is a follow on development from the FLASH system. The system has the transceiver mounted in a pod and a more compact and user friendly operator console together with improved signal handling and data storage.

This paper will show examples of lidar performance mainly from FLASH data.

THE FLASH SYSTEM

Table 1 summarises the system parameters for the FLASH system. A more detailed description is found in reference 2 and 5. Figure 2 shows a system block diagram and Figure 1 the system installation in the helicopter.

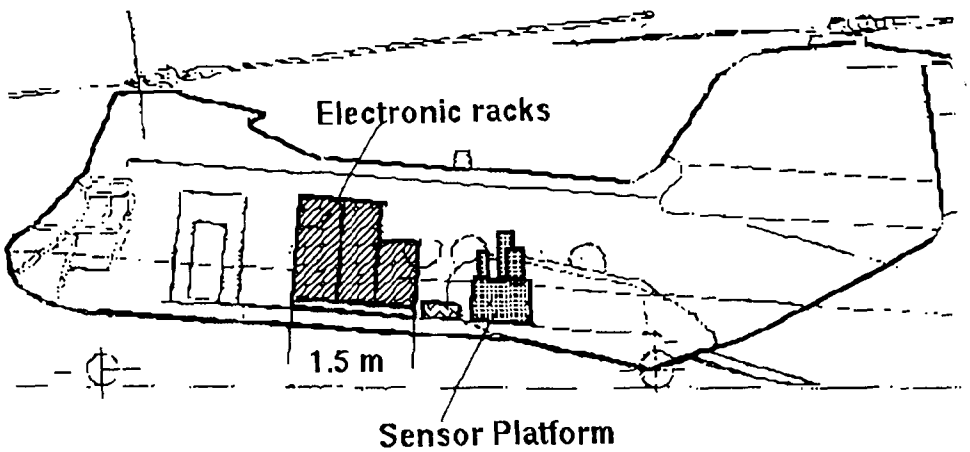

FIG. 1.- The FLASH system installation.

Table 1. FLASH system parameters.

Laser:
- Nd:YAG, 1,06 and 0,53 μm
- Prf 200 Hz, Pulse energy 3-5 mJ
- FWHM 7 ns.

"Green" receiver:
- PMT, 20 cm telescope, filter 1,2 nm
- FOV outer 5-50 mrad, inn. bl. 0- 10 mrad

"IR" receiver :
- Coax. with green, av. photo diode,
- Land/water discriminator.

Rec. Electronics:
- Log. amplifier: 80 dB.
- Le Croy digitizer: 2,5 ns sampling at 8 bits.
- Constant fraction discr. for slant range.
- Slant range resolution 8 cm.
- Real time echo extraction.

Scanner:
- Programmable, semicircular scan pattern at 20°. angle of inc. in normal mode.
- Hovering mode: ± 20° in y (^ nose dir.)
- +35° / -5° in x (in nose dir.)

Storage:
- Data: Sensor parameters, navigational data.
- Full waveforms every 6th wave form at 200 Hz, all wave forms at 62 Hz.
- Video recorder.

Navigation:
- Motorola mini ranger later replaced by GPS.

Presentation:
- Wave form, depth coded colour display

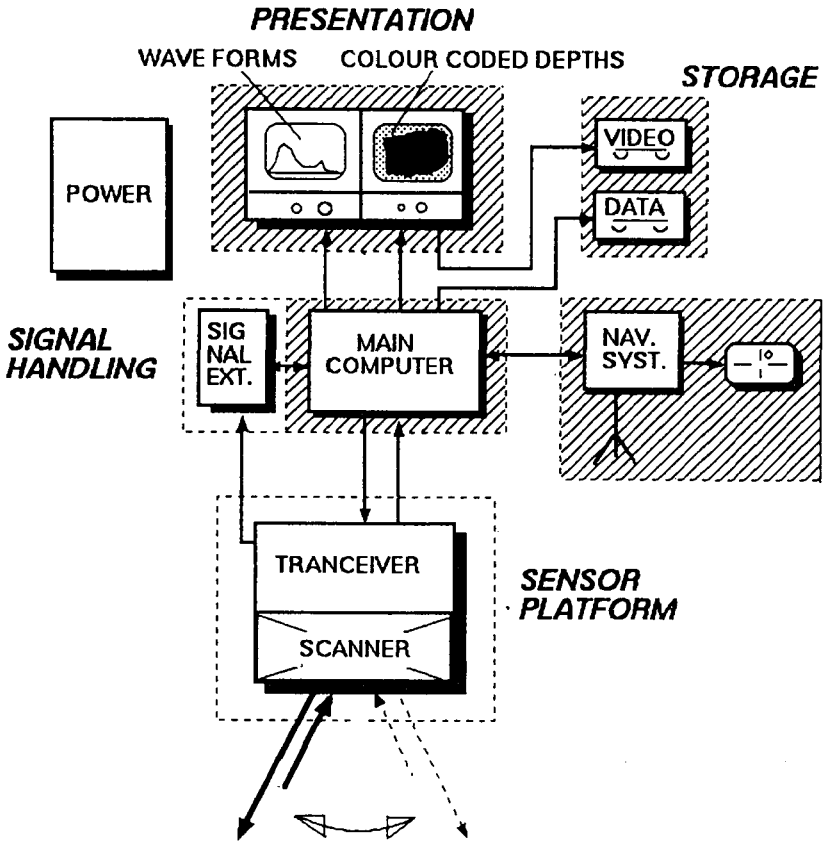

FIG. 2.- Block diagram of the FLASH system.

THE HOSS SENSOR

The profiling instrument called HOSS (Hydro Optical Sensor System)[6] is designed to be operated from a helicopter or from a ship. HOSS collects data during its up and down movement at a vertical speed of 0.5 m/s.The optical sensors measures daylight attenuation (K), beam attenuation (c), single scatter (s) and back scatter (β). From the absorption (a) and the albedo (ω_0) may be derived.

RESULTS

HOSS-measurements.

Figure 3 shows an example of HOSS- profiles.

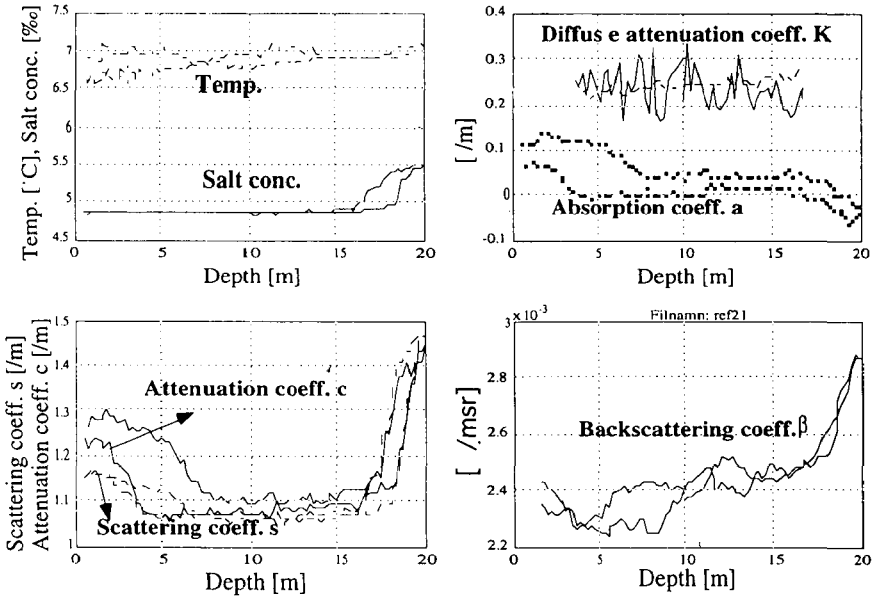

FIG. 3.- Example of HOSS profiles. The absorption a is calculated as the difference between c and s and the curves for a indicates an error in s which is estimated to 40%.

Figure 4 shows examples of correlation between the diffuse attenuation K and the total attenuation coeff. c. The similarity between different years support the fidelity of the measurements and the use of empirical relations from a certain region to estimate the maximum penetration and other performance measures of the laser system.The maximum depth penetration is for a large receiver field of view (FOV) diameter well correlated with K as shown in Figure 5.

The measure of K thus gives a good indication of the attainable depths in a certain area. The water turbidity is also depending on the time of the year and the short term weather history (esp. storms). In the inner part of the archipelago the difference in water quality varies to a larger extent with the time of the year compared to the outer parts as is shown in Figure 6.

The water back scattering properties are important as that determines the effective water reflectivity and the ability to see smaller bottom features. The back scattering coefficient scales with the scattering coefficient although the rather large

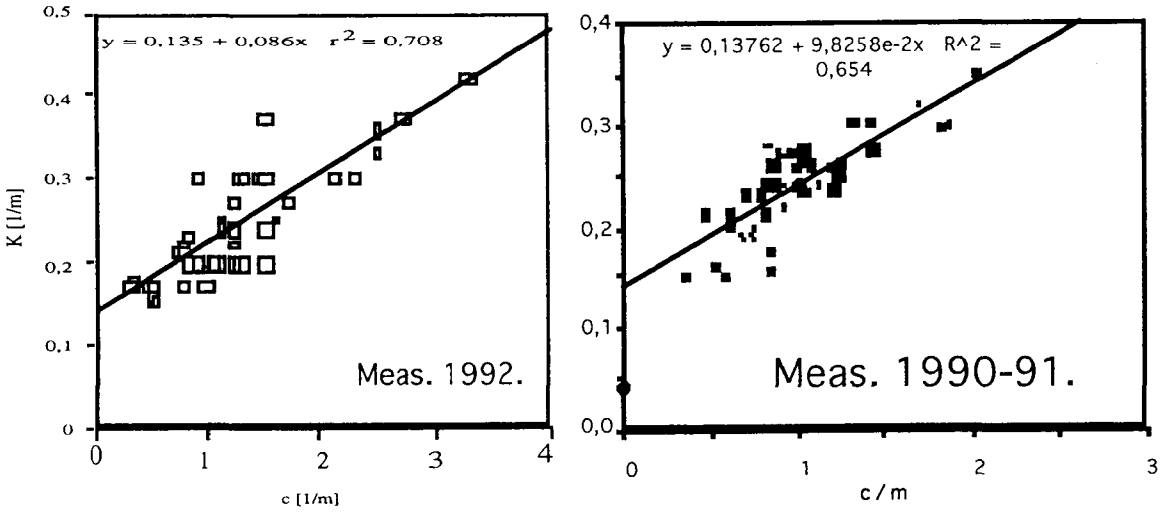

FIG. 4.- Examples of correlations of water parameters. The diffuse attenuation K which is a good measure of laser penetration is shown vs. attenuation c. Data from two separate periods.

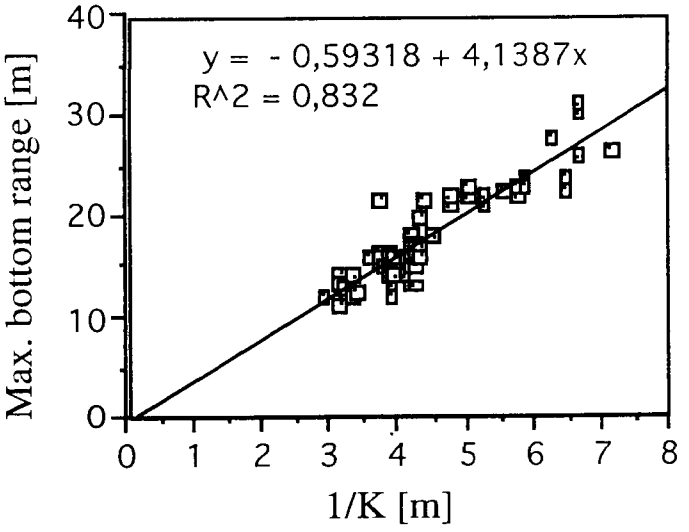

FIG. 5.- Maximum bottom range (Rb) scales approximately as Rb= 4,14/K.

spread in the data for ß vs. s indicate some instrument uncertainty in the s measurements. See Figure 7.

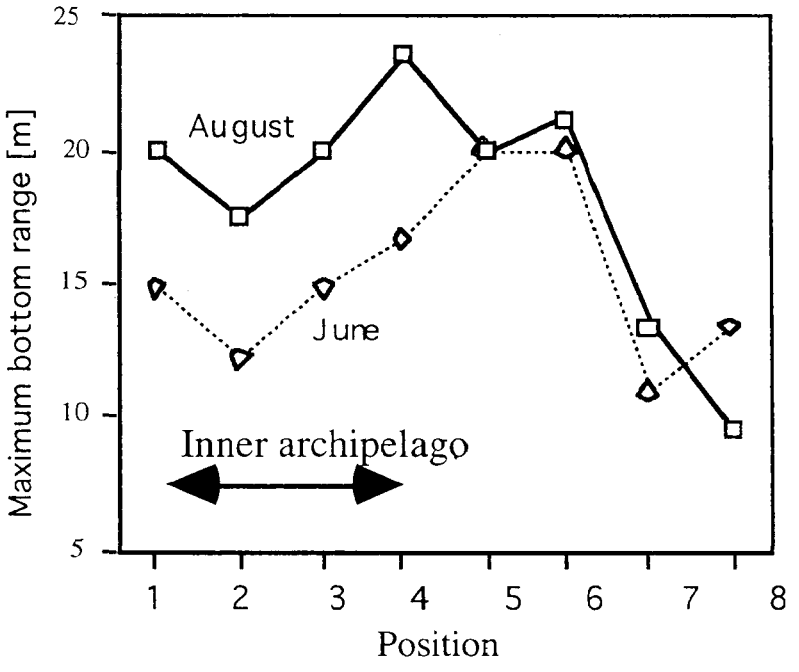

FIG. 6.- Example of range performance
at the same locations during two summer months.

Wave form analysis

Using Scan View

Some examples of wave form analysis will now be given, which is of importance for learning about the system performance for different bottoms and during different environmental conditions.

Figure 9 shows an example of data using the post processing software Scan View[9]. The colour coded swath (in grey here) is similar to the real time view of the operator. In this example we can see a dredged shoot across the flight direction. One can then choose to enlarge specific parts of the swath and double click on specific pixels to get the underlying wave form, echo classification and other relevant sensor or helicopter data associated with that laser shot.

Angle of incidence effects- surface return

The angle of incidence will affect the detected depth and the bottom echo amplitude. During some of the swaths it was noticed that there was a depth bias between the left and right parts of the swaths. Figure 8 shows examples of wave forms from different parts of the swath. The wave form consist of an artificial surface marker that is positioned in time about 1 meter (depending on PMT voltage) above the true surface and which is controlled by the slant range measurement made by

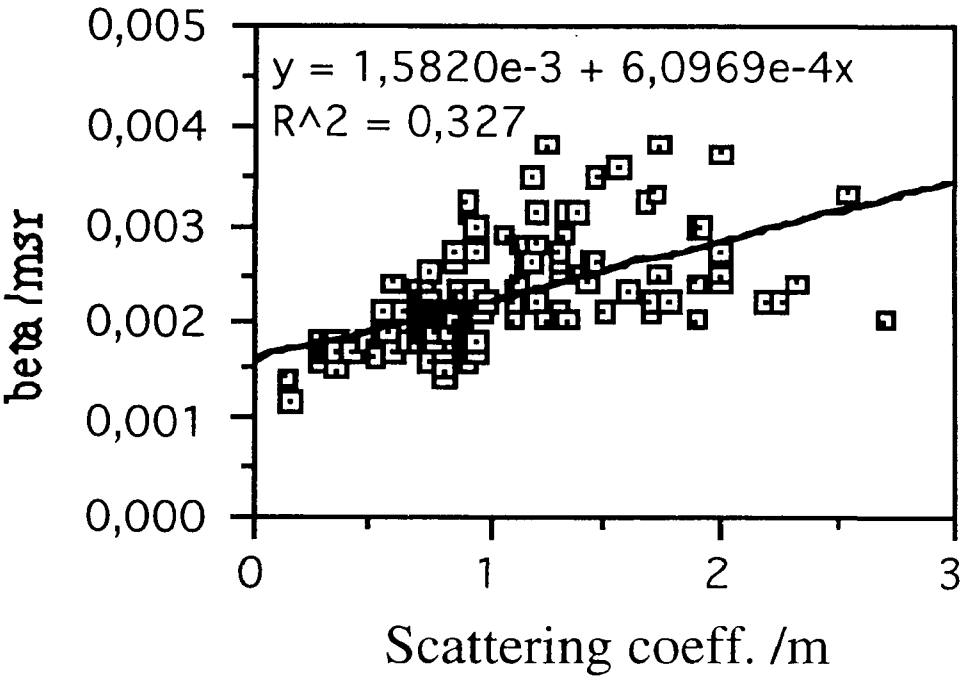

FIG. 7.- HOSS measurements of back scattering coefficient β plotted against the scattering coefficient s.

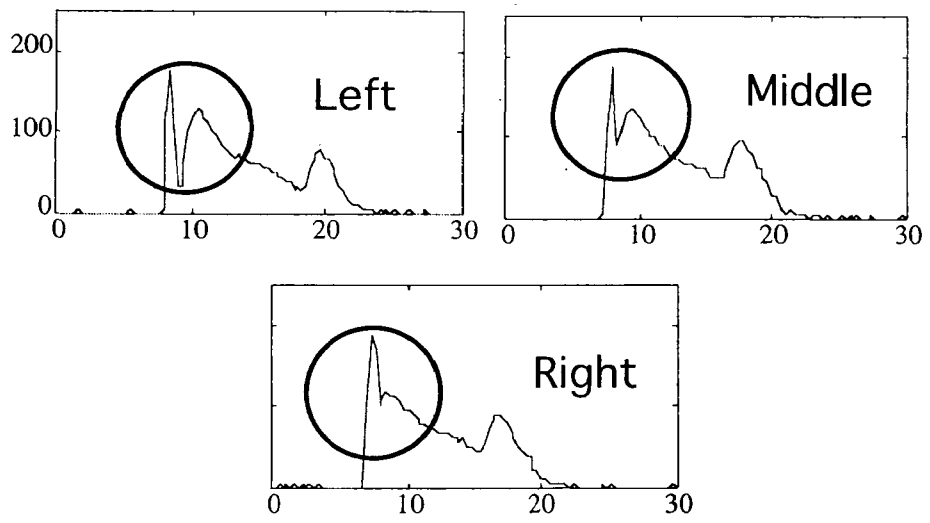

FIG. 8.- Waveforms from different parts of the swath. Note the time difference between surface marker and the green return.

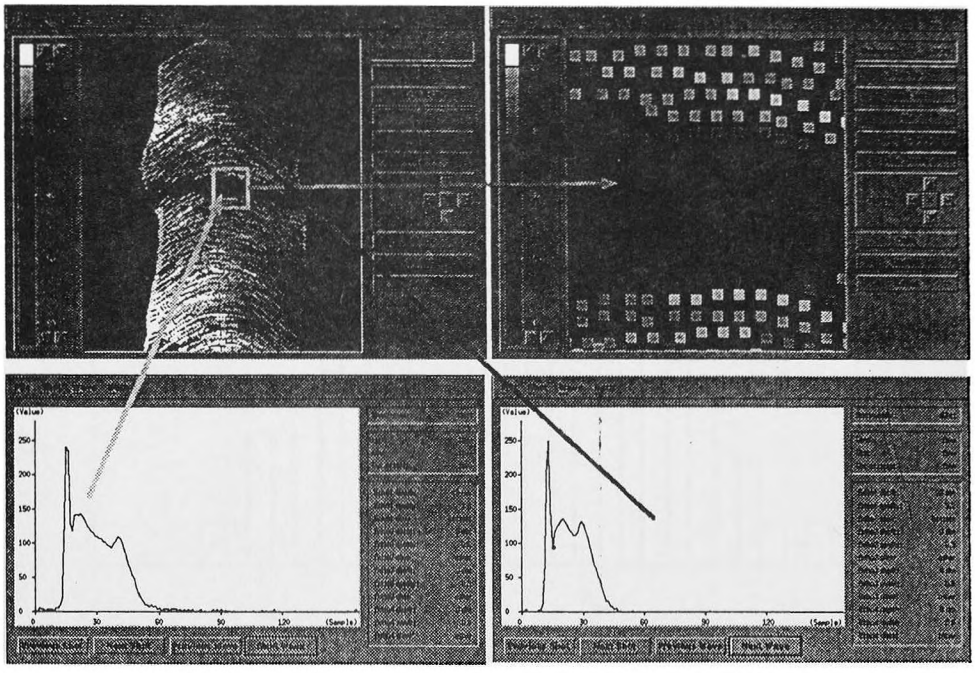

FIG. 9.- FLASH data. Upper left shows the real time swath with colour coded depths (between 2 and 7 m in this example). Right shows an enlargement for detailed investigation and below specific wave forms obtained by double clicking on pixels.

the 1,06 µm channel. As the real time echo extractor picked the "true surface" from the position of the surface peak, the variation between that peak and the position of the beginning of the green wave form will result in depth variations. As this phenomena has not been seen more than a few times it was concluded that one possible explanation might be due to surface waves that affected the IR- or green return differently depending on angle of incidence and flight direction relative to the wave propagation. The angle of incidence will also affect the magnitude of the IR-return. During calm conditions IR- dropout may occur which also affects the depth accuracy as the surface wave form of the green return might be either specular or coming from a volume return just below the surface. This "flip-flop" effect[10] can theoretically be about 0.5 meter for K-values between 0.1-0.3 m^{-1}.

Detected depth-angle of incidence

In order to investigate these effects the hydrographers advised of an area with very little depth variation. Three different areas were chosen at 6.5, 12.5 and 16.5 metres respectively. The helicopter was hovering over those areas. When analysing the data it was noted that only the area at 12.5 m was horizontal enough for further analysis so we restricted the following analysis to that depth. After post processing about 82 % of the returns were accepted as good and "solid". Figure 10 shows the measured depth distribution.

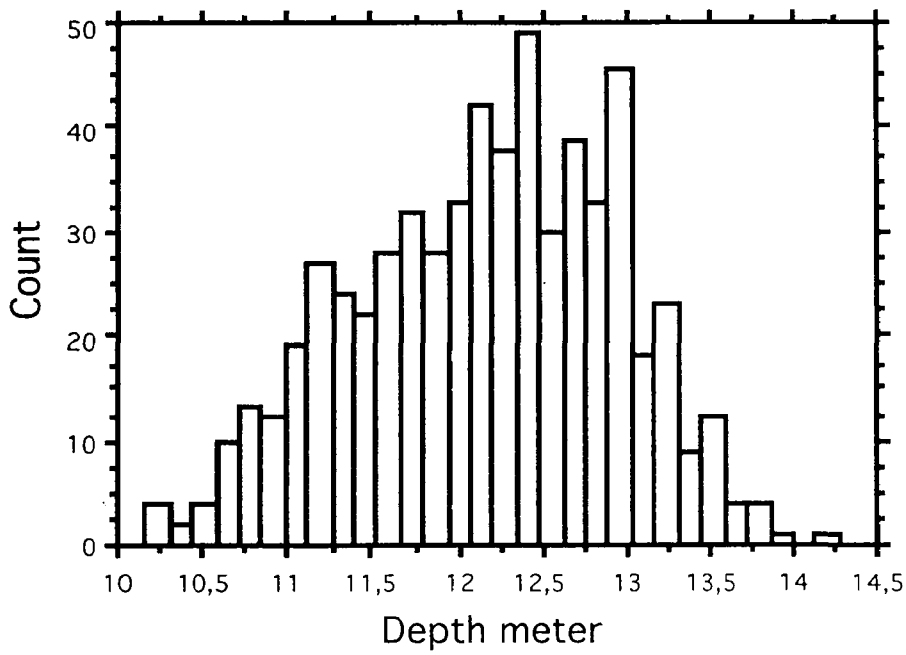

FIG. 10.- Depth distribution for the "12.5 m" test area.

Statistical tests (using ANOVA) were then made about the hypothesis that the detected depths did not depend on the scanner angles being either in X (in helicopter nose direction),Y or nadir. Figure 11 shows detected depths and bottom echo contrast (echo amplitude divided by back scatter / noise level if no echo should be present). If the test by Bonnferroni/Dunn is used it will be found (at 0,5% level of significance) that there are no significant differences in detected depth for the angle variation in X direction but significant differences in echo contrast. In the Y direction significant differences for both depths and contrast are found. For the total angle of incidence relative to nadir significant differences in both depth and contrast will be found, although the depth variation is smaller for this case than for the Y direction. This supports the assumption that there is a small bottom slope in the Y direction.

If the results with theoretical simulations are compared it will be found that very small depth differences as a function of scanner angle (about 10 cm) should be expected but we find that the contrast should change. To the first approximation there is a difference for the shortest water paths of 3 % at an angle of incidence of 20 degrees, which means less than 0.4 m for this data set. However this is compensated for when calculating the depth. The contrast difference is however larger than what should be expected from this small depth difference. The effect of slant angle of incidence is here to "stretch" the echo from the broadened beam. This effect is also seen when performing wave form simulations as shown in Figure 12. The simulated contrast decay with angle of incidence is somewhat smaller than those measured. This might be explained by the way the contrast is measured from the experimental wave form. The slope of the back scatter curve is extrapolated "below"

the bottom echo to give the contrast value. The theoretical wave form simulations are based upon the analytical formulas for beam propagation by Lutomirski[11].

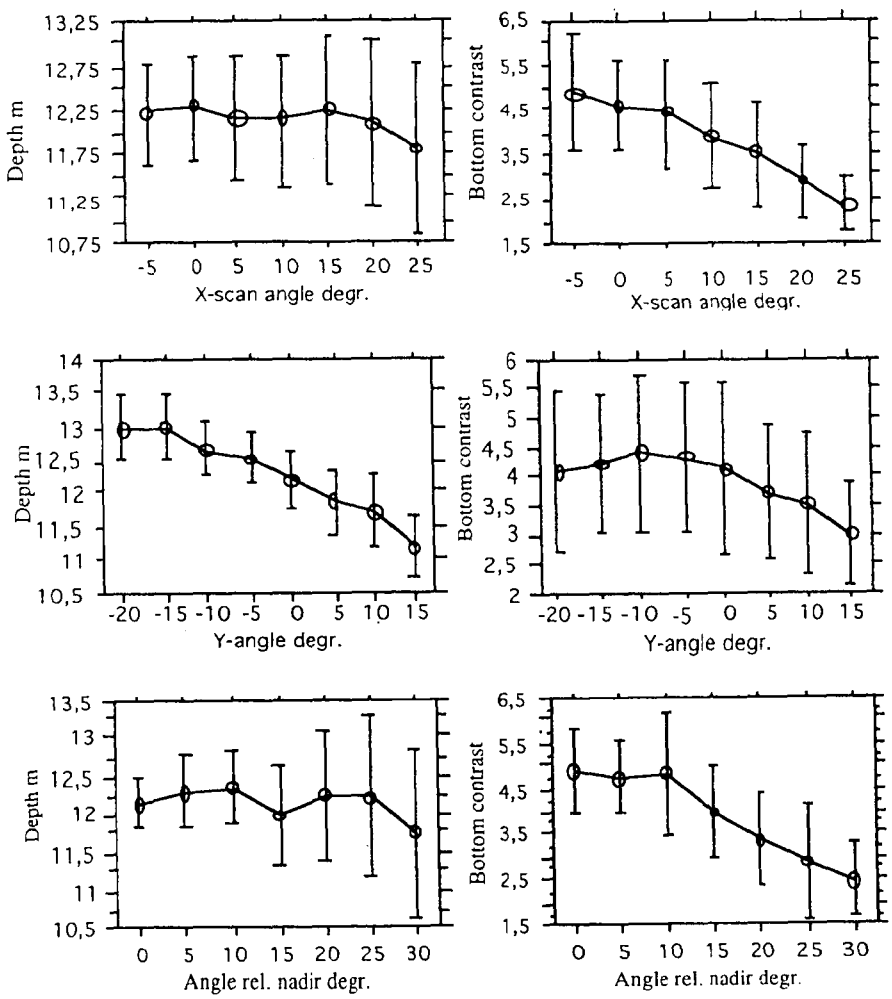

FIG. 11.- Detected depths and bottom echo contrast for different scanner angles for a rectangular scan during hovering. Av. water parameters: K=0.17/m, s=0.32/m, c=0.45/m, β=0.0017/msr.

The results found here rises the question of using smaller scanner angles (narrower swaths) to ensure depth penetration and small feature detection. A contrast decay of a factor 2 corresponds approximately to 1-3 m in depth for K between 0.3-0.1 m^{-1}.

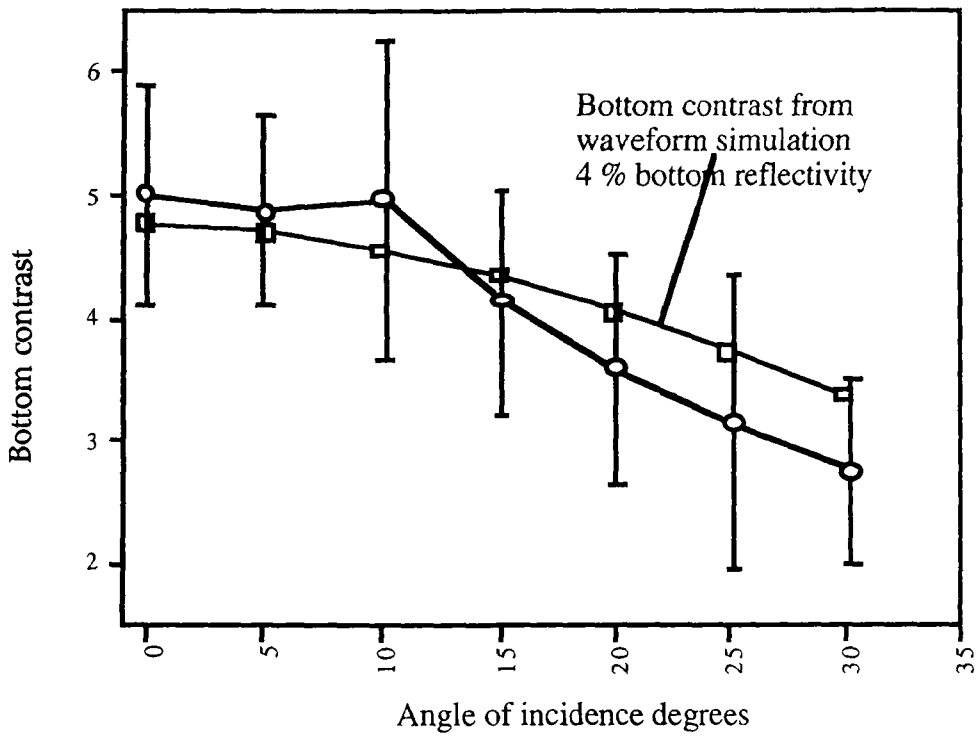

FIG. 12.- Comparison between measured and simulated bottom contrast for different angle of incidence.

Field of View (FOV) effects

The field of view of the receiver can affect the horizontal resolution of the lidar which is especially of interest for very irregular bottoms. Normally the FLASH system operates at 300 m altitude and with 50 mrad outer FOV (15 m FOV diam. at surface) and no inner blocking. The inner blocking is useful to suppress the strong returns from the surface and the layer just below. We thus found it motivated to investigate the FOV effects on the bottom contrast, detected depth, system attenuation and time parameters of the pulse. The typical number of pulses within each FOV set is about 100.

Figure 13 shows the results for detected depth and bottom contrast as a function of FOV. We have chosen data from hovering above a 50•50 m^2 area at 12.5 m depth and believed to be flat and horizontal. The water parameters were: K=0.17 /m, s=0.32 /m, c=0.45 /m, b= 0,0017 /msr. The ANOVA tests does not support any significant effects on bottom depths and contrast versus the used field of views. Error sources are scan angle effects and bottom variations.

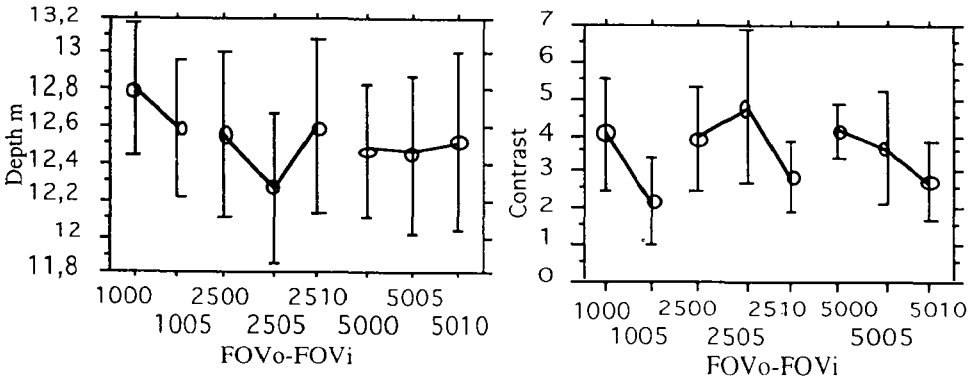

FIG. 13.- Detected depth and bottom contrast for combinations of outer field of view and inner blockings. Key: 2510 = 25 mrad FOVo and 10 mrad inner blocking.

The system attenuation G is depending on the FOV as pointed out by GORDON[12] and in an earlier paper by the author (ref.2). Figure. 14 shows G for various FOV combinations. As expected the attenuation increases with smaller FOV or larger blocking. In this water the decrease of FOV from 48 to 8 mrad (corresponding to a surface diameter of 14.4 to 2.4 m) and no inner blocking according to GORDON's article should result in a system attenuation between (0.15-0.17) to (0.23-0.27) depending on the choice of scattering phase function. The authors measured 0.162± 0.010 to 0.228±0.007 which compares rather well with the theoretical results.

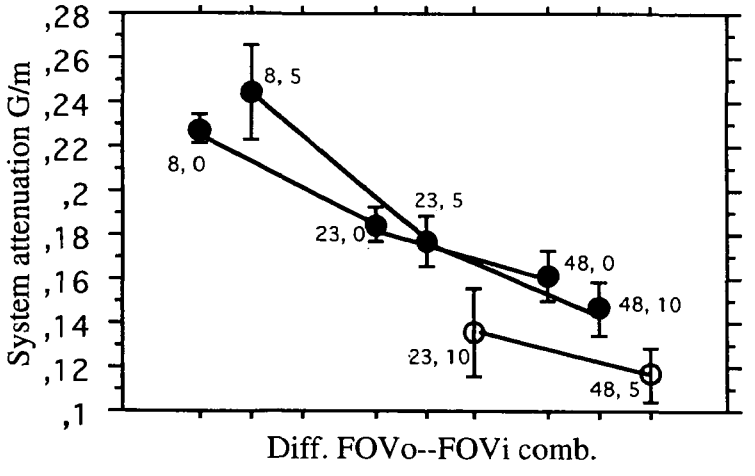

FIG. 14.- System attenuation (obtained from back-scatter slope) for various combinations of outer field of view and inner blockings.

Figure 15 finally shows the rise time and the half width of the bottom echo as a function of FOV combinations. The rise time was fairly independent of FOV but the half width shows a slight increase with the effective FOV of the receiver as should be expected.

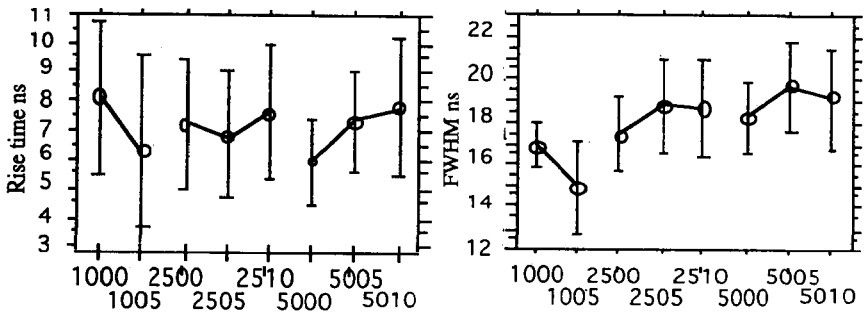

FIG. 15.- Rise time and half width versus combinations of outer field of view and inner blockings.

The choice of FOV above stony bottoms

A few comments on the influence of FOV when measuring above stony bottoms. Look at the situation in Fgure 16. A stone (assume the size1•1•1 m^3) is situated at different distances x from the projected beam center at surface. Figure 16 shows the detected depth vs stone position x. As one can see this depends to a large extent on stone position.

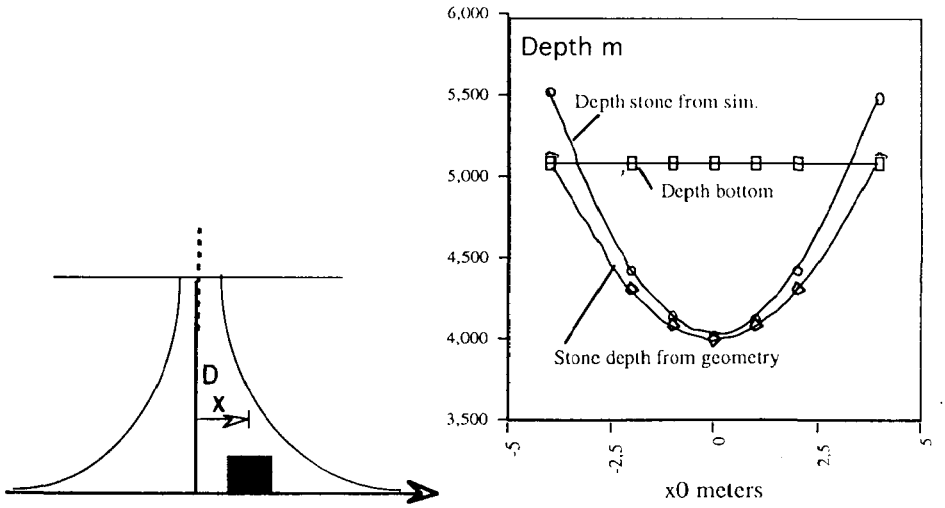

FIG. 16.- Shallowest detected depth for different stone positions x obtained by wave form simulations as compared with the shortest geometric depth between the beam and stone centre. Stone 1•1•1 m^3 on a 5 m bottom.

If the outer FOV (no blocking assumed) is altered,, the detected depth and contrast obtained by wave form simulation is shown in Figure 17. We can see that theoretically we can detect the shallowest depth if we have a threshold just above the noise level . On the other hand it is necessary to use a small FOV to have enough contrast to ensure detection of the stone. Thus there is an operational choice between FOV and horizontal resolution on one side and maximum depth penetration on the other.

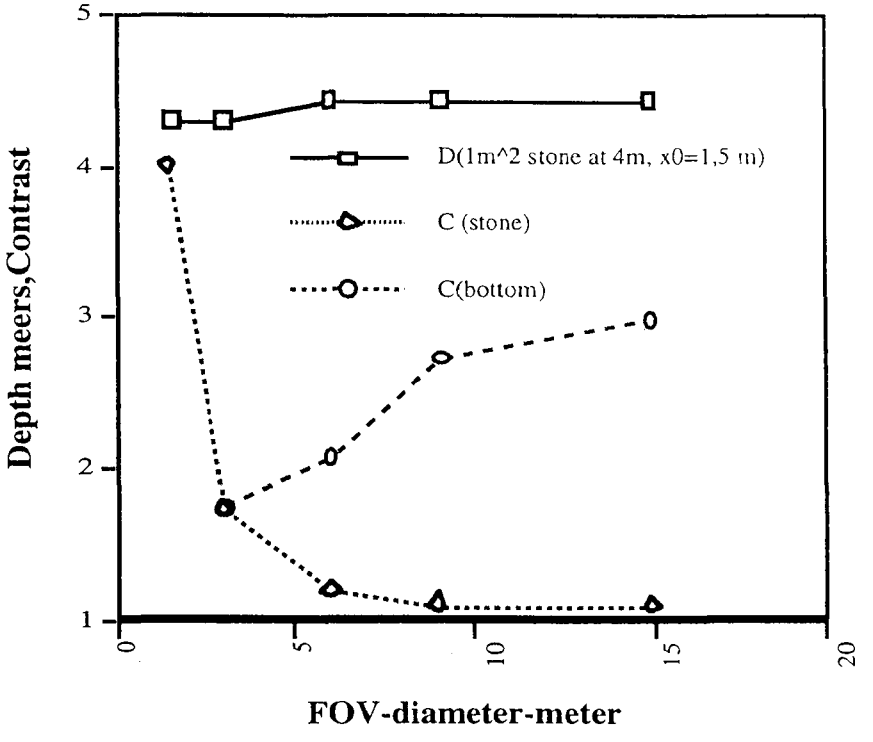

FIG. 17.- Detected depth and contrast vs receiver field of view diameter (FOV-diameter). 1•1•1 m^3 stone on a 5 m bottom and deplaced x0=1.5 m from beam centre at the water surface. Note the sharp increase of detectability (contrast) for small FOV-diameters.

Comparing contrast and G in two waters

The estimate of water turbidity is of interest for later corrections in the software processing. For large FOV diameters the system attenuation is very close to K. There are several ways of estimating G from the lidar data. One is to use the back scatter decay, another is to use the bottom decay and a third method uses the maximum range. The last two methods can obviously be combined. The back scatter decay method has the advantage of not needing any echo and can thus be applied to many wave forms such as those from deep water. However, the simple exponential decay relies on the assumption of homogeneous water in depth. This is not always the case as is illustrated in Figure 18.

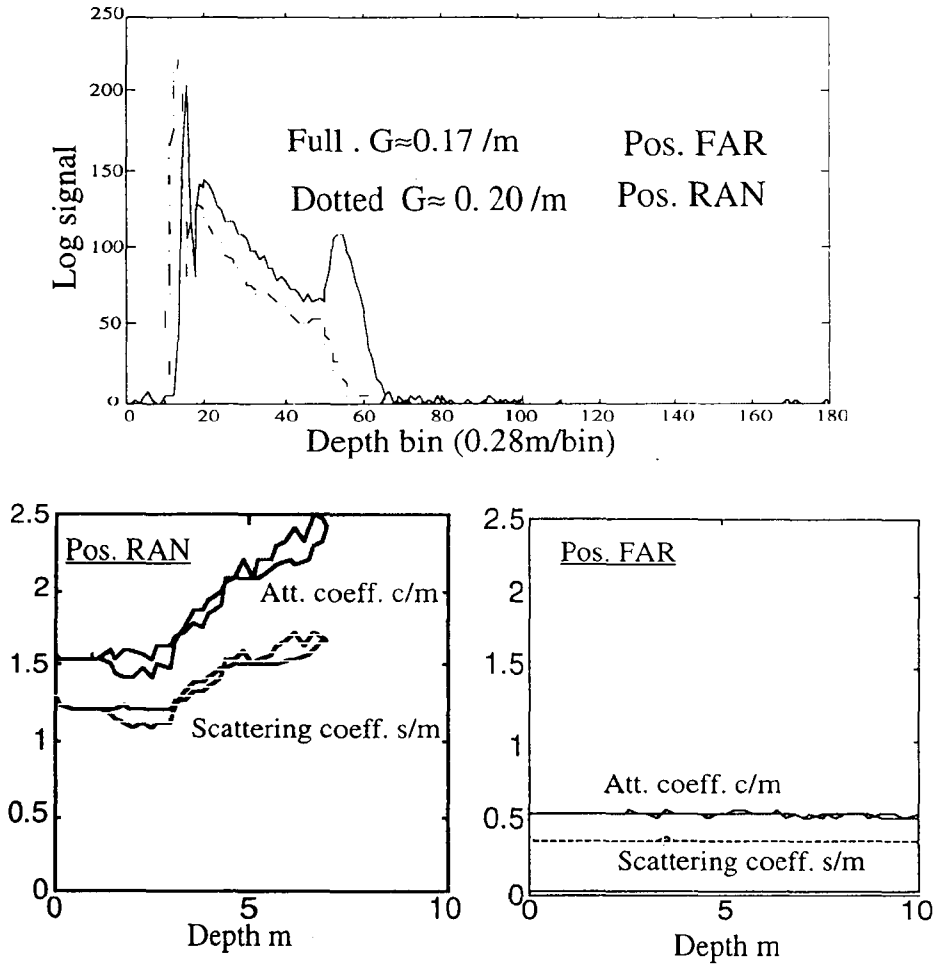

FIG. 18.- Wave forms from two water types. Measurement of G from back- scatter gives a value of G = 0,17 /m for the clear water (FAR) in acc. with depth range. In the other example (RAN) the back scatter decay heavily underestimates G 0.20 /m instead of 0.30 /m because the turbidity is not homogenous with depth as indicated by the profiles obtained by HOSS.

The great difference in bottom contrast for the echoes in the two examples of water in Figure 19 may be noted. Figure 20 shows this contrast difference for the depths 6, 8, 10 and 12 meters. As the contrast to a first approximation is given by the ratio between bottom and equivalent water reflectivity ($\rho_w = \pi\beta c_w \tau/2$, with $c_w/2\tau$ = depth interval related to laser pulse and b= backsc. coeff.) the results in Figure 20 indicate a factor of 3-4 difference in bottom reflectivity between the sites F and R as the factor in back scatter was measured to be ≈ 2 and the total contrast ratio according to Figure 19 is = 7-8.

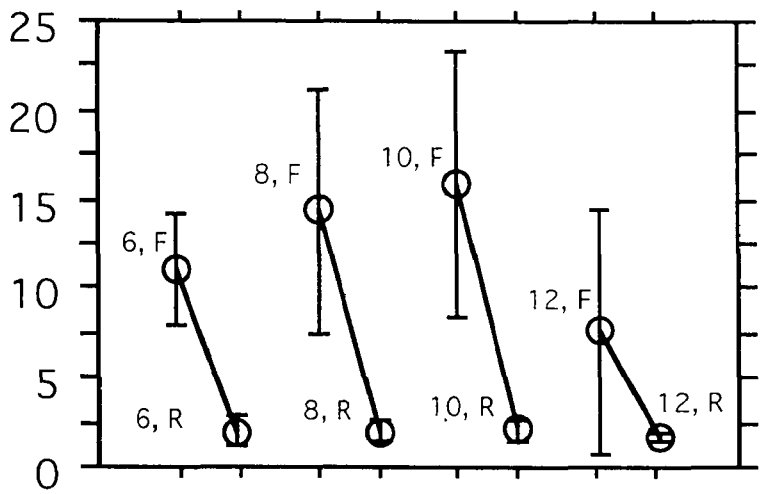

FIG. 19.- Bottom echo contrast at different depths (6 , 8, 10 and 12 m) for the sites with water clarity according to Figure 18.

Depth sounding

In collaboration with the Swedish Hydrographic Department there has been a number of campaigns to investigate the charting performance of the laser system. Most of the analysis has been done by the hydrographers and reported separately from the work of FOA. Comment will be provided shortly on some of the results.

Comparison laser-acoustic data

Before comparing the laser and acoustic data it should be noted that the FLASH system was not a total bathymeter in many aspects. For example, FLASH did not save all wave forms and the real time echo extractor was not intended for accurate depth measurements. Further there was no inertial reference system which makes wave height compensation very difficult and reduces the positioning accuracy of the helicopter. All these drawbacks have been taken into account in the Hawk Eye system.

Figure 20 shows examples of acoustic and laser data. In general the laser data looks "noisier" which might depend on the rather noisy real time echo extractor. There is not at the time of writing any knowledge of how the acoustic data have been handled.

In Figure 21 a comparison of one laser and one acoustic profile is made. The depth difference is quite small.

Figure 22 shows a comparison between laser and acoustically generated depth data. The agreement is good with a small offset of 17.8 cm. The deviation is larger at large depths where the laser approaches the max. range level. We can also note larger deviations for 4-6 metres depth.

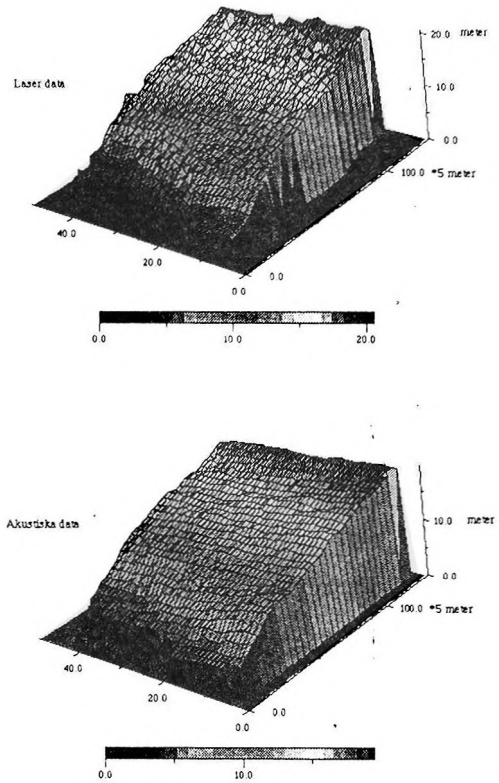

FIG. 20.- Comparison between laser and acoustic depth soundings.

Repeatability

In general problems of positioning the helicopter were encountered due to problems with the logging of GPS data. Therefore the repeatability is as much a test of the positioning accuracy as the depth accuracy. In Figure 23 the deviation between the two flight directions are rather small.

Some aspects of planning and flying

The relation between flying speed V, swath width S, laser prf f and spot density a is $V \bullet S = f \bullet a^2$. For spot densities a=5 m and S=200 m for example a 200 Hz laser gives V=25 m/s which is rather low for a helicopter making its flight wind sensitive. Therefore the planning of a mission must include consideration of the wind velocity in setting up the flight lines. It is best to fly against the wind to make it easy to hold steady course. The wind can cause the helicopter to turn more towards the wind which causes the scanner to sweep a narrower swath a bit to the side of that planned. There may be a trade off between swath width S, spot density a and the helicopter velocity V. If the speed is low relative to wind this may result in "gaps" in the coverage. The cloud base may also affect the swath width. Lower altitude means that a narrower swath can be used and enables higher flight speed for constant spot density.

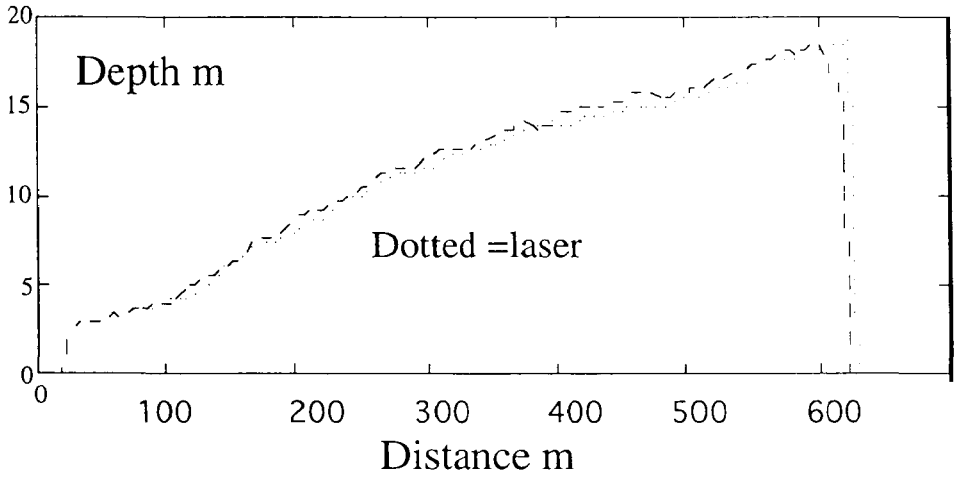

FIG. 21.- Comparison between one laser and one acoustic profile. Dotted refers to laser and hatched to acoustic data.

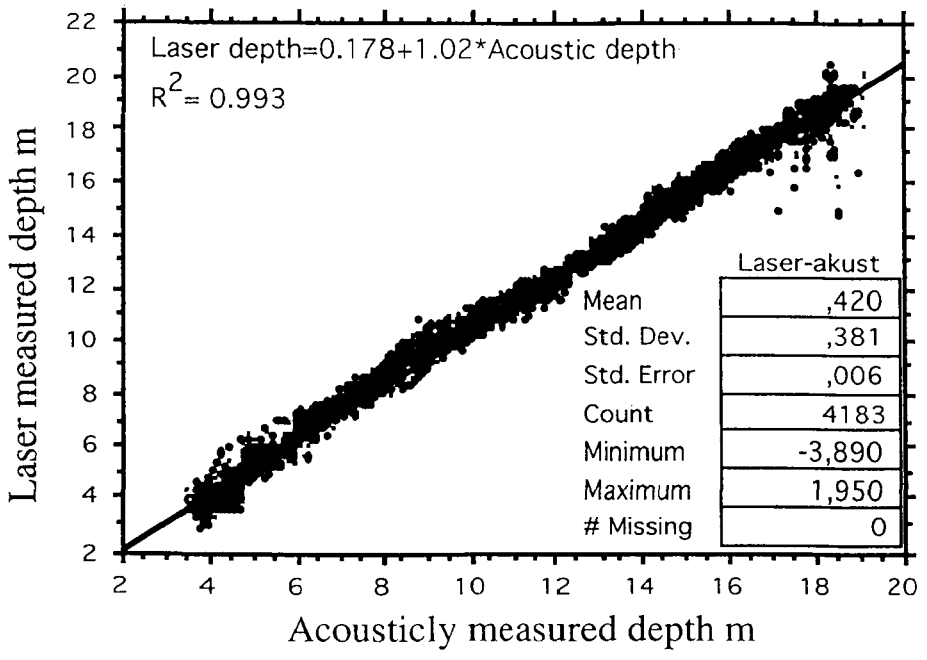

FIG. 22.- Comparison between acoustic and laser generated depths.

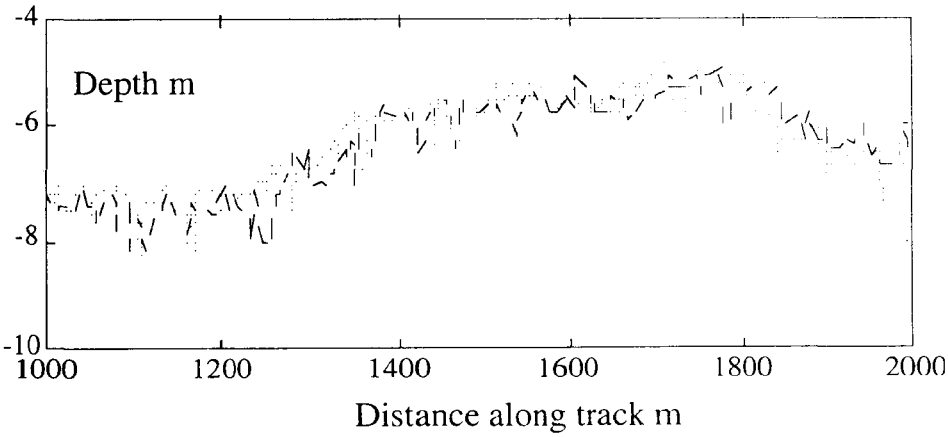

FIG. 23.- Comparison between laser data from opposite flight directions to check repeatability.

Other activities

The FLASH system has also been tested for measuring tree heights and land profiles. The results showed that both tree heights, stand volume and cutting removal could be estimated from laser height profiles. Trials have also been performed with gated viewing to increase horizontal resolution.

The Hawk Eye system

The FLASH system has been further developed into two operational systems called Hawk Eye (Figure 24). As mentioned before these systems are intended to be more suitable for accurate depth sounding. The main differences include:

- Pod mounted transceiver system
- Better wave form sampling (10 bits, 1ns)
- Storage of every wave form
- Better signal handling especially for echo extraction
- Better scanner accuracy
- Inertial reference system plus GPS
- More compact and easy installation
- Built in planning and mission software
- PMT replaced by APD for the green channel

Saab Instruments is the main contractor and Optech Inc. is the main subcontractor for the Hawk Eye. Data from Hawk Eye will hopefully be available at the time of the meeting and will be discussed. At the time of writing only data from the shake down flights are available.

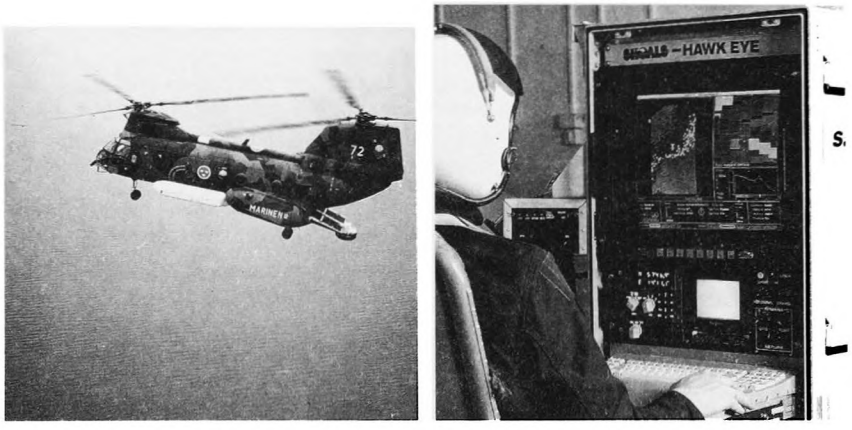

FIG. 24.- The Hawk Eye System. Left the pod mounted on a Boeing Vertol and right operator's consol. (Photo Saab Instruments).

Acknowledgements

The FLASH system was developed under contract from the Swedish Material Administration (FMV) and the interaction with FMV Radar, Optronics Section in Stockholm and FMV Testing Directorate in Linköping is greatly acknowledged. The never ending support from the Swedish Navy Staff and the 11. Helicopter Division has been of great value. The collaboration with the Swedish Hydrographic Department has been very inspiring. Finally we want to thank our subcontractors Optech Inc., Saab Instruments and AWA as well as other collegues at FOA.

Bibliography

1. O. STEINVALL et al. "Laser depth sounding in the Baltic Sea", Appl. Optics vol. 20, No. 19, pp. 3284-86, Oct. 1981.

2. O. STEINVALL, K. KOPPARI and U. KARLSSON "Experimental evaluation of an airborne depth sounding lidar", Optical Engineering, vol. 32, no. 6, pp. 1307-21, June 1993.

3. S. SVENSSON, C. EKSTRÖM, B. ERICSSON and J. LEXANDER, "Attenuation and scattering meters designed for estimating laser system performance", vol. 925, pp. 203-212, 1988.

4. O. STEINVALL et al. "Laser depth sounding in the Baltic Sea", FOA report C 30219-E 1 May 1981.

5. R. AXELSSON, O. STEINVALL and P. SUNDBERG, "Programmable scanner for laser bathymetry", International Hydrographic Review vol. 67, no.1, pp.161-170, January 1990.

6. S. SVENSSON, C. EKSTRÖM, B. ERICSSON and J. LEXANDER, "Attenuation and scattering meters designed for estimating laser system performance", SPIE Proceedings Ocean Optics IX, vol.925, pp. 203-212, 1988.

7. T. KAISER ,"Computer simulations of laser bathymetry ", National Defence Research Institute (FOA) report FOA C 30517-3, 1 Dec. 1988.

8. O. STEINVALL, K. KOPPARI and U. KARLSSON, "Simulation of lidar bathymetry results from irregular bottom", FOA report in manuscript.

9. S. KULLDORFF, "Scan View-A graphics program for laser bathymetry analysis", FOA report C 30707-3.1, 1993.

10. GUENTHER G.C., MESICK H.C., "Automated Lidar Waveform Processing" Proceedings US Hydro Conference April 12-15, 1988, Baltimore, USA.

11. R.F. LUTOMIRSKI, "An analytical model for optical beam propagation through the maritime boundary layer", pp. 110-122, SPIE Ocean Optics V, vol.160, 1978.

12. H.R. GORDON,"Interpretation of airborne oceanic lidar effects of multiple scattering", Applied Optics, vol.21, no.16, pp. 2996-3001, August 1982.